The Relative Biological Effectiveness of Low-Dose Mammography Quality X Rays in the Human Breast MCF-10A Cell Line

Caitlin E. Mills,[a,1] Christopher Thome,[a] David Koff,[b] David W. Andrews[c,1] and Douglas R. Boreham[a,d,2]

[a] Department of Medical Physics and Applied Radiation Sciences, [b] Department of Radiology, [c] Department of Biochemistry and Biomedical Sciences, McMaster University, Hamilton, Ontario, Canada; and [d] Northern Ontario School of Medicine, Sudbury, Ontario, Canada

Mills, C. E., Thome, C., Koff, D., Andrews, D. W. and Boreham, D. R. The Relative Biological Effectiveness of Low-Dose Mammography Quality X Rays in the Human Breast MCF-10A Cell Line. *Radiat. Res.* 183, 42–51 (2015).

Mammography is used to screen a large fraction of the population for breast cancer, and mammography quality X rays are speculated to be more damaging than the higher energy X rays used for other diagnostic procedures. The radiation dose delivered to breast cells as a result of these screening exposures may be a concern. The purpose of this current study was to determine the relative biological effectiveness (RBE) of low-energy mammography X rays for radiation-induced DNA double-strand breaks evaluated using a highly sensitive automated 53BP1 assay. Automation of the 53BP1 assay enabled the quantification and analysis of meaningful image-based features, including foci counting, within the cell nuclei. Nontumorigenic, human breast epithelial MCF-10A cells were irradiated in the low-dose range with approximately 3–30 mGy of 29 kVp mammography X rays or ^{137}Cs (662 keV) gamma rays. The induction and resolution of the 53BP1 foci did not differ significantly between exposures to ^{137}Cs gamma rays and 29 kVp X rays. The RBE was calculated to be 1.1 with a standard deviation of 0.2 for the initial number of radiation-induced double-strand breaks. The radiation dose from a single mammogram did not yield a significant change in the number of detectable foci. However, analysis of additional features revealed subtle differences in the distribution of 53BP1 throughout the nuclei after exposure to the different radiation qualities. A single mammogram was sufficient to alter the distribution of 53BP1 within the nuclear area, but not into discrete foci, while a dose-matched gamma exposure was not sufficient to alter the distribution of 53BP1. Our results indicate that exposure to clinically relevant doses of low-energy mammography quality X rays does not induce more DNA double-strand breaks than exposure to higher energy photons.   © 2015 by Radiation Research Society

INTRODUCTION

Mammography is used worldwide to screen for and diagnose possible breast cancer. Specific, optimal screening recommendations are frequently debated and modified; thus, interest in the effects of the radiation dose associated with one, or repeated scans is persistent. The Canadian Task Force on Preventive Health Care recommends that routine screening for women with average breast cancer risk commence at age 50 and be repeated at 2–3 year intervals until age 74 (*1*). Similar guidelines exist in the United States (every 2 years from age 50 −74), the United Kingdom (every 3 years between ages 50–70) and Australia (every 2 years from age 50–69) (*2–4*). The biological effects of these repeated low-dose radiation exposures are important to understand given that breast tissue is considered by some to be radiosensitive. The International Commission on Radiological Protection (ICRP) recently (2007) increased the tissue weighting factor (W_T) of the breast from 0.05 (*5*) to 0.12 (*6*).

Mammography delivers a low dose of low-energy X rays to detect areas of high-density tissue within the breasts. X-ray tube voltages from 24–35 kVp are commonly used, with molybdenum or rhodium targets and filters (*7*). The doses delivered depend on the settings and design of the machine being used, as well as the size and tissue composition of the breast being examined (*7*). For the most part, radiation doses are lower with digital mammograms (1.2–1.9 mGy per view) compared to film mammograms (approximately 2–2.4 mGy per view), thus radiation exposure from mammography has decreased as more digital units have been introduced (*7, 8*). This trend of decreasing dose has evolved since the 1960s when the average glandular dose was between 12–15 mGy depending on breast thickness (*9*). The Canadian Mammography Quality Guidelines (*10*) and the U.S. Food and Drug Administration's Mammography Quality Standards Act (*11*) require that the average glandular dose per view not exceed 3 mGy under specified parameters.

A number of groups have sought to determine the relative biological effectiveness (RBE) of mammography quality X rays. One approach is the current radiation weighting factor

TABLE 1
The RBE of Mammography Quality X Rays Relative to ^{137}Cs Gamma Rays Based on 53BP1 Foci

Radiation quality	Slope (excess foci/mGy)	Uncertainty	R^2
^{137}Cs γ rays	0.0141	0.0008	0.993
29 kVp X rays	0.015	0.002	0.971
RBE	**1.1 ± 0.2**		

Notes. The slopes (with associated standard deviations) for the induction of 53BP1 foci with respect to dose for the reference, gamma radiation and query, mammography X rays, exposures shown in Fig. 2. The RBE and standard deviation, which were determined based on these values, are also included.

used for radiation protection purposes for all photon exposures (*12*). However, there are physical reasons to suggest that low-energy X rays may be more damaging than higher energy photons. In general, the linear energy transfer (LET) along a photon track is inversely related to its energy: the more energetic the photon, the more energetic the secondary electrons, the fewer ionizations per track length on average (*13, 14*). Thus it follows that lower energy X rays could result in more complex DNA lesions, including DSBs, at the cellular level (*13*). However, the predominant mechanism of interaction between an incident photon and its target shifts from Compton scattering to the photoelectric effect as the photon energy decreases from approximately 200 keV to 26 keV, by which point the interactions are almost entirely photoelectric (*12, 15*). This is an important consideration for mammography quality X rays because the complete energy transfer associated with their photoelectric interactions yields secondary electrons with energies similar to those generated by 200 keV X rays through Compton scattering. Therefore, the RBE of mammographic X rays [unrestricted dose mean LET ~4.3 keV/μm at 30 kVp (*14*)] with respect to approximately 200 keV X rays [unrestricted dose mean LET ~3.5 keV/μm (*14*)] should be close to unity. Nonetheless, since mammography X rays are not monoenergetic, those at lower energies would result in higher LET secondary electrons, which could in turn produce a slightly higher RBE. Microdosimetric work by Brenner and Amols (*16*) and Kellerer (*14*) suggested RBE values of 1.3 and less than 2, respectively. Currently, there is no consensus in the literature as to the RBE of mammographic irradiation, because different cell lines, end points, reference radiation qualities and dose ranges have been used in these studies resulting in estimates ranging from ~1–8 (reviewed in Table 2). We sought to evaluate the effects of mammography quality X rays relative to gamma rays from a ^{137}Cs source using a clinically relevant cell line, end point and dose range.

The 53BP1 assay was used for high-content analysis of radiation-induced foci, to directly investigate the RBE of exposures as low as those from a single mammogram. Given the uncertainty surrounding the shape of the radiation dose-response curve in the low-dose range, it is important to collect data directly in the low-dose range in an appropriate

cell line. The fact that the RBE is known to be dependent on dose, dose rate and cell line further underscores this need (*12*). Thus, directly measuring low, clinically relevant doses should provide more valuable insight into the effects of mammography at the cellular level than extrapolating from data collected at high doses, or in nonbreast cell lines. The 53BP1 assay is used to quantify DNA double-strand breaks (DSBs), which are the critical lesions of radiation-induced damage in cells. By comparing the initial changes in 53BP1 between cells exposed to mammography X rays and ^{137}Cs gamma rays, the capacity of each radiation quality to induce critical DNA lesions was investigated.

MATERIALS AND METHODS

Cell Culture

MCF-10A cells, human breast epithelial cells, were selected for this study because they are genomically stable, and despite being immortalized, are nontumorigenic and exhibit traits of normal human breast epithelial cells in culture. MCF-10A cells were maintained in 1:1 Dulbecco's modified Eagle medium F12 (DMEM/F12) (Life Technologies™, Burlington, Canada) with 5% horse serum (Life Technologies), 10 μg/ml insulin (Sigma-Aldrich, Oakville, Canada), 0.5 μg/ml hydrocortisone (Sigma-Aldrich), 20 ng/ml epidermal growth factor (R&D Systems™, Burlington, Canada), 100 ng/ml cholera toxin (Sigma-Aldrich) and 1% penicillin-streptomycin (Life Technologies). The cells were incubated at 37°C and 5% CO_2. They were subcultured approximately twice per week at 1:3–1:5 ratios.

Irradiation and Dosimetry

Cells were seeded (4,000 cells per well) in 50 μl media in 384 well tissue culture treated cell carrier plates (PerkinElmer Inc., Woodbridge, Canada) and allowed to adhere for 24 h prior to irradiation. All plates (one control plate per time point, X and gamma irradiated) per experimental replicate were seeded at the same time and irradiated on the same day. The plates were placed in an ice slurry (0°C) 20 min before radiation exposure. Plates were irradiated with the lid on and a layer of media approximately 0.5 cm thick above the cells. Postirradiation, all plates were returned to 37°C and incubated for the desired amount of time before being fixed without a media change.

Cells were irradiated with ^{137}Cs gamma rays (662 keV) using the McMaster University Taylor Radiobiology Source. The plates were kept on ice for the duration of the exposures to mitigate dose-rate effects and control incubation and repair times post exposure. For the mammography exposures, the cells were irradiated with a clinical General Electric Senographe Essential digital mammography unit (GE Healthcare, Milwaukee, WI). X rays (29 kVp) were delivered using a rhodium target, rhodium filter and a tube current–exposure time product of 63 mAs. The nominal focal spot size was 0.3 mm, and a breast thickness of 45 mm was assumed for the machine based dose readings. The cells received 1, 3 or 10 consecutive mammograms. The plates were removed from ice and placed on the supporting table for these very short exposures, and returned to the ice slurry immediately afterwards. The compression paddle was removed from the mammography unit for these exposures.

The GE mammography unit provided values for the entrance surface exposure (ESE) and average glandular dose (AGD) of 5.2 mGy and 1.38 mGy, respectively, based on the exposure settings used and the predicted attenuation properties of breast tissue. Thermoluminescent dosimeters (Harshaw TLD-100 LiF chips, K&S Associates Inc., Nashville, TN) were used to verify the doses delivered to the cells in 384 well plates. Five chips were arrayed, on the bottom of 384 well plates containing 50 μl of water per well, to determine spatial

MILLS *ET AL.*

TABLE 2
Summary of RBE Values for Mammographic X Rays in the Literature

Source	Doses	Mammography	Reference	Cells used	End point	RBE
Heyes and Mill (*21*)	0.27–6.08 Gy	29 kVp	A-bomb spectrum, 2.2 MeV β particles	CGL1 (HeLa × fibroblast hybrid)	Neoplastic transformation	4.42 ± 2.02
Frankenber *et al.* (*22*)	1–6 Gy	29 kVp	200 kVp X rays	CGL1	Neoplastic transformation	4.67 ± 3.93
	1–5 Gy	29 kVp	200 kVp X rays	CGL1	Survival	4.38 ± 1.87
	Suggested	29 kVp	^{60}Co γ rays	CGL1	Neoplastic transformation	~8
Goggelmann *et al.* (*23*)	1–5 Gy	29 kVp	220 kVp X rays	CGL1	Neoplastic transformation	3.58 ± 1.77
Schmid (*24*)	0.05–4 Gy	29 kVp	220 kV X rays	Human lymphocytes	Dicentric chromosomes	1.64 ± 0.27
	0.05–4 Gy	29 kVp	^{60}Co γ rays			4.75 ± 1.67–6.12 ± 2.51
Gomolka *et al.* (*25*)	0.5–3 Gy	29 kVp	^{60}Co, ^{137}Cs γ rays, 220 kV X rays	Human lymphocytes	Single-strand breaks (Comet assay)	None calculated, no significant changes found
Brenner (*26*)	0.25–1 Gy	15–25 keV	^{137}Cs γ rays	C$_3$H10T1/2	Oncogenic transformation	<2.5
Kuhne *et al.* (*19*)	4–20 Gy fractions	29 kVp	^{60}Co γ rays	Primary human fibroblasts	DSB induction via PFGE	1.15 ± 0.05
Mestres *et al.* (*27*)	0.05–3 Gy	30 kVp	120 kVp X rays	Donor blood	Translocations and dicentrics via FISH	1.51 ± 0.47 (translocations) 1.73 ± 0.59 (dicentrics) 1.42 ± 0.41 (breaks)
Lehnert *et al.* (*28*)	0.5–10 Gy	25 kV	200 kV X rays	MCF-12A	Clonogenic survival, micronuclei	Dose dependent 1.13 ± 0.03 (survival 100 mGy) 1.44 ± 0.17 (MNi)
Beyreuther *et al.* (*29*)	0.5–5 Gy	25 kV	200 kV	184A1	Chromosome fragments	1.17 ± 0.12
				MCF-12A		0.97 ± 0.10
Panteleeva *et al.* (*30*)	1–6 Gy	25 kV	200 kV	HEKn	Clonogenic survival	1.81 ± 1.1
Depuydt et al. (*20*)	0.01–2 Gy	30 kV	^{60}Co γ rays	Peripheral blood lymphocytes	γ-H2AX foci and micronuclei	1.36 (foci) 0.95–1.98 (95% CI) 1.44–7.5 (micronuclei)
Frankenberg-Schwager *et al.* (*31*)	0.25–2 Gy	29 kVp	200 kVp X rays	MRC5-CV1	HPRT gene mutations	2.7 ± 0.2
Virsik *et al.* (*32*)	0.17–4.63 Gy	30 kV	150 kV	Human lymphocytes	Dicentric chromosomes	1.25–3
Slonina *et al.* (*33*)	1–5 Gy	25 kV	200 kV X rays	Human keratinocytes	Micronuclei	1.3
	1.04–5.2 Gy	25 kV	200 kV X rays	Human fibroblasts	Micronuclei	1.2
Kellerer (*14*)	–	30 kVp	200 kVp X rays	Calculation based	Theoretical estimates	<2
Brenner and Amols (*16*)	–	23 kVp	250 kVp X rays	Calculation based	Theoretical estimates	1.3
	–	23 kVp	A-bomb γ spectrum	Calculation based	Theoretical estimates	2
Verhaegen and Reniers (*17*)	–	~28 kVp	300 keV X rays	Calculation based	Monte Carlo simulations	<2
Bernal *et al.* (*18*)	–	28 and 30 kVp	^{60}Co γ rays	Calculation based	DNA DSB by Monte Carlo	1.3 ± 0.1
This work	**0.003–0.03 Gy**	**29 kVp**	**^{137}Cs γrays**	**MCF-10A**	**53BP1 foci**	**1.1 ± 0.2**

Notes. The doses and end points studied, as well as the reference radiation used, are included for comparisons. The results obtained from the current work are included at the bottom of the table.
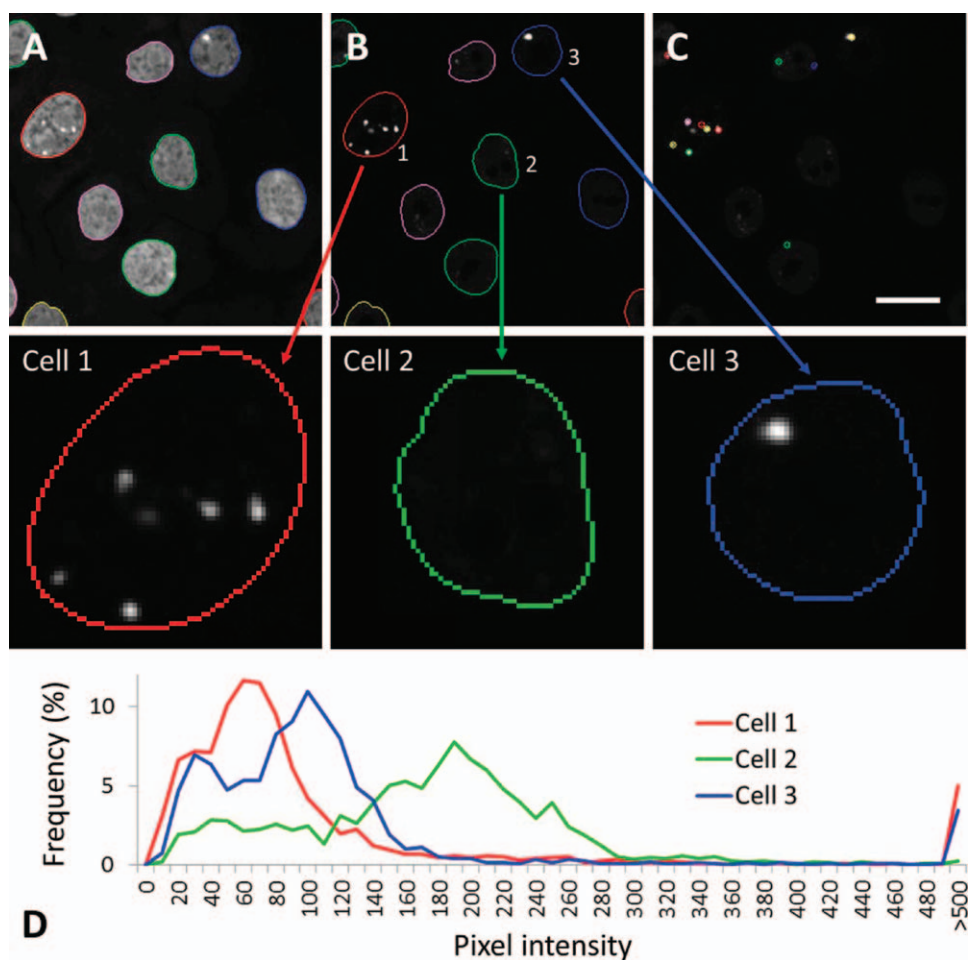
FIG. 1. Panel A: Segmentation of nuclei of MCF-10A cells stained with DRAQ5. Panel B: The nuclear mask was overlaid on the 53BP1 image. Panel C: Foci detection was limited to the nuclear area. The foci that were identified are outlined. The panels labeled: Cell 1, Cell 2, Cell 3 are magnified and their 53BP1 staining shown. Panel D: The intensity of each pixel within the nuclear area was measured. The distributions of these intensities are plotted for Cells 1–3.

variability in the dose rate across the plate. One plate was given ten mammograms, which corresponded to 29 ± 2 mGy or 2.9 mGy per scan. To verify previously calibrated (measured with a Farmer 2570 dosimeter with a 0.6 cc ion chamber) dose rates on the Taylor source, a second plate was exposed for 3 min 34 s at a distance of 150 cm from the source, corresponding to a dose of 46 ± 1 mGy or 12.9 mGy/min. The combined expanded uncertainty of the TLD measurement process was 5% for a single TLD (K&S Associates), which was incorporated in the uncertainties listed above. Rh/Rh30 and Rh/Rh35 National Institute of Standards and Technology (NIST) calibration beams were used for the TLD based mammography dosimetry. The absolute response of the TLDs was within 0.5% for both calibration beams. A ^{137}Cs beam was used for calibration for the Taylor source exposed TLDs.

53BP1 Immunofluorescence

A Thermo-Scientific SP-Workcell comprised of a central Vertical Array Loader (VAL) robotic arm (Thermo-CRS, Waltham, MA), two Multidrop™ Combi liquid dispensing units (Thermo Scientific, Waltham, MA), two BioTek ELx405™ plate washers (Winooski, VT), a Hamilton STARlet liquid handling platform (Reno, NV) and an ABgene plate sealer (Thermo Scientific). Briefly, the cells were fixed in 4% paraformaldehyde for 20 min, permeabilized with 1% Triton™

X-100 for 15 min, blocked with 3% bovine serum albumin (BSA) for 60 min, then incubated with primary mouse anti-human 53BP1 (1:1,500 in 1.5% BSA) for 90 min (BD Biosciences, Mississauga, Canada), followed by Alexa Fluor® 562 secondary antibody (1:1,500 in 1.5% BSA) for 60 min (Life Technologies, Burlington, Canada). Lastly, the nuclei were stained with 1.5 μ*M* DRAQ5 (Biostatus, Shepshed, UK) at least 30 min prior to imaging. All solutions were prepared in phosphate buffered saline (PBS).

Imaging and Analysis

Images of at least five fields of view (40× water immersion objective) per well were acquired with an Opera® high throughput spinning disk confocal microscope (PerkinElmer Inc.). The DRAQ5 signal was used to segment the images (nucleus, cytoplasm and whole cell masks were defined) using built-in nuclear and cytoplasm detection algorithms in Acapella® software (PerkinElmer Inc.). Figure 1A shows an example of nuclear segmentation. Any cells that touched image borders were excluded from analysis. The nuclear borders that were defined, using the DRAQ5 signal, were applied to the 53BP1 image and analysis of foci was restricted to those nuclear areas (Fig. 1B). An existing Acapella spot detection algorithm was used for foci identification and quantification (Fig. 1C). Segmentation and spot detection were optimized by adjusting
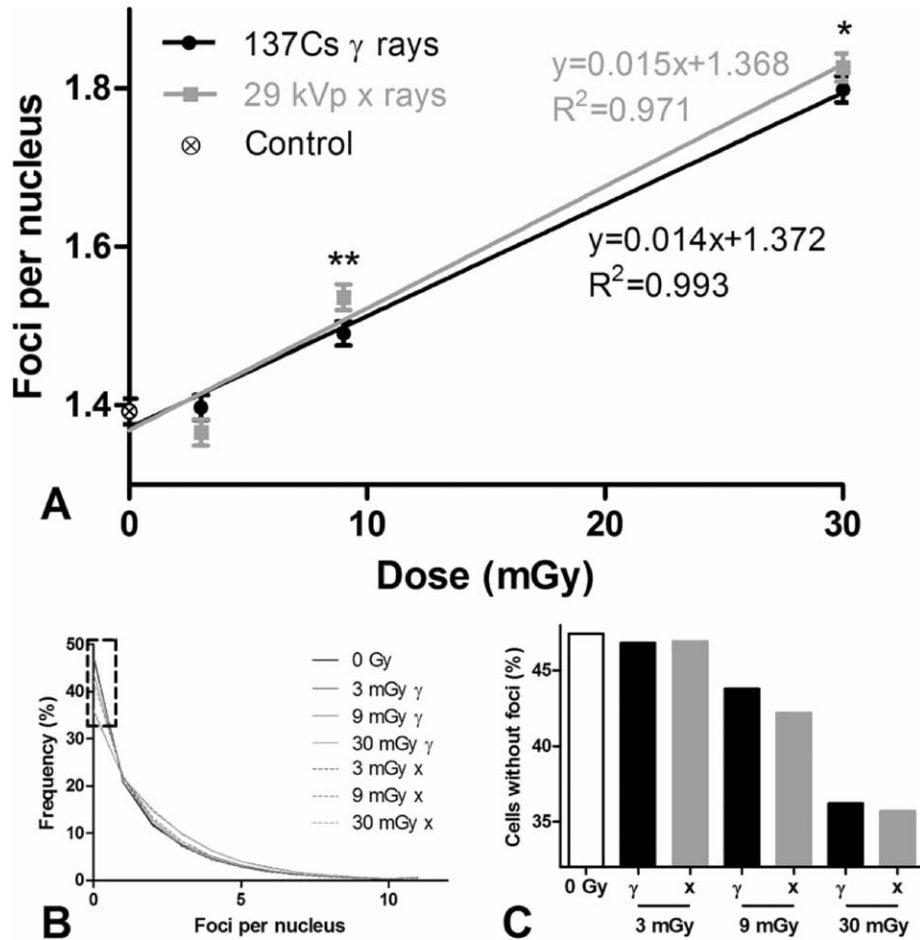
FIG. 2. Panel A: The number of 53BP1 foci 1 h post exposure to low-dose ^{137}Cs gamma rays or 29 kVp mammography quality X rays. Each point represents the mean of at least 57,000 cells from three independent experiments, and the error bars represent the 95% confidence intervals. Panel B: The object level frequency distribution of 53BP1 foci per cell for each treatment. The region within the dotted rectangle highlights the frequency of cells without detectable foci 1 h after the indicated exposures and is shown in panel C. *Treatments resulted in significantly more foci than control levels; **the radiation qualities also differed. All frequency distributions were significantly different from control except those of the 3 mGy treatments. The distributions at 9 mGy differed between radiation qualities (KS test, $P < 0.01$).

intensity and contrast thresholds. All foci were counted at all dose points. Results are presented as the average number of foci per nucleus, or as the average number of excess foci per nucleus in which cases the average number of foci detected in the nonirradiated control cells was subtracted from the averages in the irradiated cells. Data are also presented as frequency distributions of foci per nucleus for all cells segmented. Beyond foci detection, morphology, intensity and texture features were quantified and compiled in a text file for each channel acquired of the nuclear mask segmented for every cell imaged. The manual analysis of features of interest was performed using Microsoft Excel (Redmond, WA) and SigmaPlot™ 11.0 (Systat Software Inc., San Jose, CA). One such feature was the standard deviation of the intensity of the 53BP1 signal, which was obtained by measuring the 53BP1 intensity of each pixel within the nuclear area and calculating the standard deviation of the values. Pixel intensity histograms for three sample cells are shown in Fig. 1D. The average standard deviation of the intensity of 53BP1 was low in cells with diffuse 53BP1 signal throughout the nucleus, and higher for those with one or more distinct foci. Cell 1 had six foci, cell 2 did not have any detectable foci and cell 3 had a single focus (Fig. 1). The bright pixels that made up the foci in cells 1 and 3 resulted

in distributions of pixel intensities with a relatively high frequency above 500 compared to cell 2 in which few pixels had intensities above 500 (Fig. 1D). Statistical analysis was performed using SigmaPlot 11.0 and MATLAB® (MathWorks, Natick, MA). One-way ANOVA was used for multiple comparisons, and the Kolmogorov-Smirnov (KS) test statistic was used to determine differences between distributions of data.

RESULTS

The RBE of 29 kVp Mammography X Rays

We used an automated 53BP1 assay to study the RBE of the radiation exposure associated with mammography. To do this, MCF-10A cells were exposed to approximately 3, 9 or 30 mGy of 29 kVp X rays delivered using a clinical mammography unit. Dose-matched ^{137}Cs gamma ray exposures were administered for the reference radiation. These doses were selected because they represent the doses associated with one, three and ten
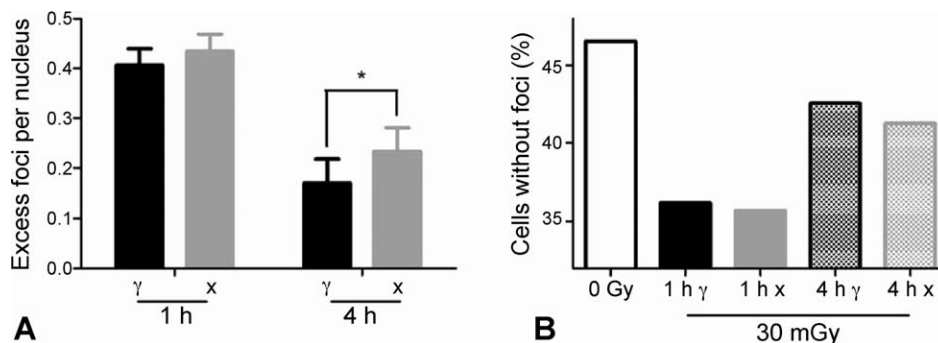
FIG. 3. Panel A: The resolution of 53BP1 foci in MCF-10A cells 4 h after exposure to 30 mGy of 29 kVp mammographic X rays or ^{137}Cs gamma rays. Panel B: The frequency of cells without detectable foci for the indicated treatments. Over 38,800 objects were scored per treatment between two biological replicates. Each point represents the mean, and the error bars represent the 95% confidence intervals. *The number of excess foci at the 4 h time point differed significantly between the radiation qualities (ANOVA, $P < 0.01$).

mammograms and therefore are clinically relevant exposures.

The dose-response curves for both radiation qualities are shown in Fig. 2A. Neither the single 3 mGy mammogram nor the 3 mGy of gamma-ray exposure yielded a statistically significant increase in radiation-induced foci in MCF-10A cells 1 h postirradiation using the automated 53BP1 assay developed in our laboratory. The increases in radiation-induced foci above control levels only reached statistical significance at 9 mGy ($P < 0.01$) in the cells treated with mammographic X rays or gamma radiation. The frequency distribution of cells with n foci is shown in Fig. 2B, and the decrease in the frequency of cells with no detectable foci with increasing dose is highlighted in Fig. 2C. These plots show the distribution of the data from all replicates comprising a minimum of 57,000 cells per treatment and as such, they do not have associated error bars. The RBE at minimal doses (RBE$_M$) is defined as the ratio of the slopes of the initial (linear) dose-response curves of the query radiation and reference radiation qualities (*12*). The mammography and gamma radiation 53BP1 response curves were both fit linearly yielding an RBE$_M$ of 1.1 with a standard deviation of 0.2 (Table 1).

Despite the RBE being indistinguishable from one within the uncertainty bounds of the experiments, subtle differences in the number of foci induced by the different radiation qualities were observed (Fig. 2A). These observations suggest that additional work at doses below 10 mGy is warranted especially for mammography quality X-ray exposures.

Repair of Mammography-Induced DNA Damage

Since it has been suggested that an enhanced RBE of mammography quality X rays would emerge downstream of the initial damage, we looked at the resolution of 53BP1 foci 4 h postirradiation. After a 30 mGy exposure to ^{137}Cs gamma rays or 29 kVp X rays, there were significantly fewer excess 53BP1 foci per nucleus at 4 h relative to the 1 h time point (Fig. 3A). Evidence of repair was also apparent

by the increase in the number of cells with no detectable foci at 4 h compared to 1 h post exposure for both radiation qualities (Fig. 3B). There was a small statistically significant elevation in the persistence of foci induced by the mammography exposure relative to the gamma exposure at the 4 h time point.

Additional Modifications in 53BP1

To determine if the changes in 53BP1 induced by exposure to mammography quality X rays differed from those induced by ^{137}Cs gamma rays, over 160 features were interrogated. Intensity, morphology and texture features were extracted for the 53BP1 and DRAQ5 channels within the nuclear area. Each dose and time point represents over 50,000 cells from three independent experiments. Ultimately the automation of the 53BP1 assay enabled the throughput of sufficiently large data sets to directly study the effects of clinically relevant low doses.

Analysis of standard deviation of the intensity of the 53BP1 signal within the nuclei was anticipated to increase with exposure to ionizing radiation, since it is representative of the redistribution of the protein from diffuse to punctate at the DNA DSB sites. Figure 4 shows a direct linear relationship between the mean of the standard deviation in the 53BP1 signal and the number of foci per nucleus in the nonirradiated control cells. This result is consistent with the localization of 53BP1 into foci generating a quantifiable increase in staining intensity at those spots subsequently increasing the standard deviation of intensity within the nuclear area (Fig. 4). This feature was measured within the automatically detected nuclear areas, therefore, it is likely to be sensitive to subtle changes that do not result in discrete foci, and was thus compared for the mammography and gamma-radiation exposed cells. The presence of any detectable foci yielded a statistically significant increase in the standard deviation of 53BP1 intensity within the nuclear area. However, it did not differ significantly for cells with over six detectable foci. It follows that this metric is only useful at low doses. Over 95% of the cells scored at all
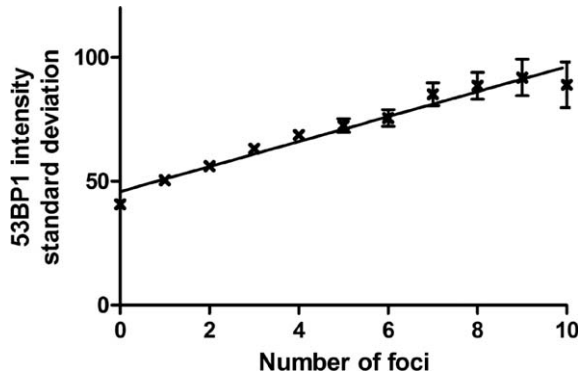
FIG. 4. The change in the standard deviation of the 53BP1 signal with respect to the number of 53BP1 foci detected per nucleus. Error bars represent the 95% confidence intervals. The increase in 53BP1 intensity standard deviation above that of 0 foci was statistically significant for all foci per nucleus counts (ANOVA, $P < 0.01$).

doses considered here had six or less detectable foci (Fig. 2B).

When the average of the standard deviation of the 53BP1 intensity was determined with respect to radiation exposure interesting differences were observed between mammography and gamma-radiation exposed cells (Fig. 5). Most striking was the effect at 3 mGy where the difference in standard deviation between the radiation qualities was evident in cells with the same number of detected foci (Fig. 5A). Although this dose did not yield a significant change in the number of foci induced by either radiation quality as measured by foci counting, the mammographic X rays induced a significant change in the average of the standard deviation of the 53BP1 intensity throughout the nuclei whereas the gamma rays did not (Fig. 5B). The effect of the mammography X rays was more pronounced at 3 mGy and 30 mGy where the qualities yielded statistically different results. Four hours postirradiation, evidence of repair (indicated by a decrease in the standard deviation of the 53BP1 intensity) was present in the cells treated with 30 mGy regardless of radiation quality (Fig. 5B).

DISCUSSION

Mammography quality radiation was not found to be more effective than gamma radiation at inducing DNA DSBs in MCF-10A cells at clinically relevant doses. The RBE of 1.1 ± 0.2 for 29 kVp X rays found here is in general agreement with the calculation based estimates of <2 for the RBE of mammographic X rays reported by Kellerer (*14*) and Verhaegen and Reniers (*17*). Our result is also in agreement, within the uncertainties, with the theoretical estimates of 1.3 and 1.3 ± 0.1 reported by Brenner and Amols (*16*) and Bernal *et al.* (*18*), respectively (Table 2). The estimates for the RBE of mammographic X rays based on DNA DSB induction presented in Table 2 are both higher than the current result. However, the RBE of 1.15 ± 0.05 reported by Kuhne *et al.* (*19*) and that of 1.36 with a 95% confidence interval of 0.95–1.98 reported by Depuydt *et al.* (*20*) both overlap with the RBE of 1.1 ± 0.2 reported here when uncertainties are considered. Based on the values presented in Table 2, it is evident that there exists a large divide in the RBE estimates for mammography quality X rays. Specifically, the highest published values are almost entirely from work performed in the CGL1 cell line and, for the most part, based on the long-term end point of neoplastic transformation. These studies have been controversial [e.g., see Redpath and Mitchel (*34*)] largely because none of them included doses in the low-dose range. In a subsequent study by Ko *et al.* (*35*), in the same CGL1 cell line using the same neoplastic transformation assay, clinically relevant doses were studied. Exposures ranging from 0.5–220 mGy of 28 kVp mammography quality X rays were administered. Doses up to 11 mGy were found to suppress transformation, whereas those from 11–220 mGy were not found to significantly alter it (*35*). Interestingly, Portess *et al.* (*36*) used a co-culture system to show that the irradiation of nontransformed 208F rat fibroblast cells with doses as low as 2 mGy (gamma rays) resulted in increased levels of apoptosis in nonirradiated transformed 208F*src3* cells. Their findings suggest that radiation exposure at clinically important levels may, under some circumstances,
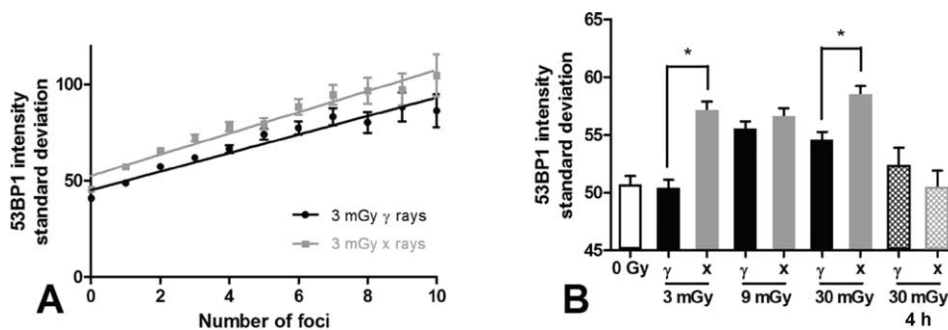

FIG. 5. Panel A: The standard deviation of the intensity of 53BP1 with respect to the number of foci detected in cells exposed to 3 mGy of gamma rays or X rays. Panel B: The average of the standard deviation of the intensity of 53BP1 signal within the nuclear area of MCF-10A cells exposed to the doses indicated. Data are for 1 h postirradiation except where noted. Each bar represents the mean of at least 57,000 objects from three independent experiments, and the error bars represent the 95% confidence intervals. *Treatments that were significantly (ANOVA, $P < 0.01$) different.

result in the selective clearance of transformed cells (*36*). Thus it is possible that mammography yields tumor suppressing, protective effects, in addition to its known benefit of early breast cancer detection.

Discrepancies in biological effects between low and high doses have been shown in DNA DSB induction. Beels *et al.* (*37*) found a biphasic relationship with low-dose hypersensitivity in γ-H2AX foci formation after 100 kVp X irradiation in whole blood samples. The slope of the dose response was 10 times higher for doses below 10 mGy compared to higher doses. Colin *et al.* (*38*) looked at γ-H2AX foci formation in primary mammary epithelial cells exposed to clinical doses of 28 kVp X rays. Damage was found to be greater from repeated low doses compared to single higher doses. These results strongly underscore the importance of collecting data at low doses, as well as the problems associated with extrapolating results from high doses for the purpose of risk estimation in the low-dose range.

Nonetheless, it is interesting to note that the assays that measured immediate, or short-term effects generally yielded lower RBE values, closer to those expected based on theoretical estimates. This has led to speculation that the differential effects of radiation quality arise at later time points postirradiation for a variety of reasons. For example, Gomolka *et al.* (*25*) suggested that damage induced by different radiation qualities is processed differently. More specifically, it has been reported that the chromosome aberrations induced by mammographic X rays are more complex than those induced by higher energy X rays (*27*), and that mammography-induced DSBs are more often misrepaired than those induced by gamma radiation (*19*). Lehnert *et al.* (*28*) observed that mammography quality X rays, compared to higher energy X rays, resulted in more cells with damage rather than more severely damaged cells. However, these findings and predictions were all based on exposures well above those that are clinically relevant. Such differences in the radiation-induced damage of varying qualities would be missed if foci were only scored immediately after the exposures, since they would likely manifest as disparities in the rate of foci resolution, where foci at the sites of more complex breaks would be more persistent.

It has been reported that DNA damage induced by low doses of ionizing radiation is not repaired as efficiently as that induced by higher doses in primary human fibroblasts because low doses do not generate enough free radicals to trigger a response (*39, 40*). Conversely, Asaithamby and Chen (*41*) reported efficient repair of DNA DSBs induced by doses as low as 5 mGy. The data presented in Fig. 3 suggest that the MCF-10A cells promptly repaired damage induced by low doses regardless of radiation quality. Despite strong evidence of repair in both the X- and gamma-irradiated cells, there were significantly more foci remaining 4 h post-mammography exposure to 30 mGy than ^{137}Cs exposure to the same dose. Similar results were

seen by Beels *et al.* (*37*) who observed persistent γ-H2AX foci at lower energy 100 kVp X rays compared to ^{60}Co gamma rays, up to 24 h after 5 and 200 mGy doses. It is possible that this subtle disparity in the repair kinetics was the result of a difference in the complexities of the induced damage. This result may warrant further attention, and future studies should focus on foci resolution over longer time periods.

Additional evidence for a difference in the effectiveness of the radiation qualities emerged from the analysis of the standard deviation of the intensity of the 53BP1 signal. These data are indicative of a threshold for the induction of 53BP1 redistribution. It appeared that once the standard deviation of the 53BP1 intensity increased (initially at 3 mGy for the 29 kVp X rays and at 9 mGy for the gamma rays), higher doses had minimal effects. It is possible that the X rays induced slightly more complex damage as a result of their higher LET relative to the gamma exposure. If this is the case, then it provides additional support for effective repair of radiation-induced damage even at low doses, and has positive clinical implications.

CONCLUSION

The RBE of 29 kVp mammographic X rays was found to be 1.1 ± 0.2 based on the automated 53BP1 foci assay. Gamma rays from a ^{137}Cs source were used as the reference radiation. Human breast epithelial MCF-10A cells were used for this work because they are nontumorigenic and possess genetic aberrations characteristic of benign and cancerous lesions, making them a good model for cells that would be routinely exposed to mammograms. Furthermore, the use of a clinical mammography unit ensured that directly relevant exposures in terms of radiation quality and dose were administered and studied.

No significant changes in the number of 53BP1 foci were detected in cells exposed to a single mammogram, however, exposures to doses equivalent to three or ten mammograms yielded significant increases in 53BP1 foci. Importantly, the damage induced by these exposures was shown to have undergone significant repair within 5 h of irradiation. Additional analysis revealed that the 3 mGy exposure to mammographic X rays, but not to γ rays, altered the distribution of 53BP1 within the nuclear area. Ultimately, the biological significance of this change in 53BP1, but not into distinct foci, is unclear and represents a potential focus for future work.

Furthermore, the results presented here show that it is possible to study the effects of clinically relevant radiation exposures directly, and our data suggest that there is no indication that mammography X rays induce more DNA DSBs than gamma radiation. Future work will focus on the long-term effects of the clinically relevant exposures studied to provide concrete data upon which risk estimates can be based. Assay automation will continue to facilitate the direct investigation of low-dose radiation exposures, which have

historically been too subtle to detect due to throughput, sensitivity and bias limitations by manual analyses, effectively reducing the need for extrapolation from higher doses.

REFERENCES

1. Canadian Task Force on Preventive Health Care. Recommendations on screening for breast cancer in average-risk women aged 40–74 years. CMAJ 2011; 183:1991–2001.

2. Screening for breast cancer: U.S. Preventive Services Task Force recommendation statement. Ann Intern Med 2009; 151:716–26.

3. National Health Service Breast Cancer Screening Programme. London: Public Health England; 2013. (http://bit.ly/1vNFwtQ)

4. Australian Government Department of Health and Ageing. National policy. BreastScreen Australia; Canberra: Commonwealth of Australia; 2010. (http://www.health.gov.au/)

5. ICRP, Recommendations of the International Commission on Radiological Protection. ICRP Publication 60. Ann ICRP, 1990; 21.

6. ICRP, The 2007 Recommendations of the International Commission on Radiological Protection. ICRP Publication 103. Ann ICRP, 2007; 37.

7. Bushberg J, Seibert J, Leidholdt J, Edwin M, Boone J. The essential physics of medical imaging. 3rd ed. Philadelphia: Lippincott Williams & Wilkins; 2012.

8. Hendrick RE, Pisano ED, Averbukh A, Moran C, Berns EA, Yaffe MJ, et al. Comparison of acquisition parameters and breast dose in digital mammography and screen-film mammography in the american college of radiology imaging network digital mammographic imaging screening trial. AJR Am J Roentgenol 2010; 194:362–9.

9. Thierry-Chef I, Simon SL, Weinstock RM, Kwon D, Linet MS. Reconstruction of absorbed doses to fibroglandular tissue of the breast of women undergoing mammography (1960 to the present). Radiat Res 2011; 177:92–108.

10. Health Canada. Canadian mammography quality guidelines. Ottawa: Minister of Public Works and Government Services Canada; 2002. (www.hc-sc.gc.ca)

11. Mammography quality standards act. Silver Spring: U. S. Food and Drug Administration; 2002. (http://1.usa.gov/1zjGajr)

12. ICRP, Relative biological effectiveness, radiation weighting and quality factor. ICRP Publication 92. Ann ICRP. 2003.

13. Goodhead DT. Initial events in the cellular effects of ionizing radiations: clustered damage in DNA. Int J Radiat Biol 1994; 65:7–17.

14. Kellerer AM. Electron spectra and the RBE of x rays. Radiat Res 2002; 158:13–22.

15. Knoll GF. Radiation detection and measurement. 3rd ed. Hoboken: John Wiley & Sons; 2000.

16. Brenner DJ, Amols HI. Enhanced risk from low-energy screen-film mammography x rays. Br J Radiol 1989; 62:910–4.

17. Verhaegen F, Reniers B. Microdosimetric analysis of various mammography spectra: Lineal energy distributions and ionization cluster analysis. Radiat Res 2004; 162:592–9.

18. Bernal M, David M, Pires E. Estimation of the RBE of mammography-quality beams using a combination of a monte carlo code with a b-DNA geometrical model. Phys Med Biol 2011; 56:7393–403.

19. Kühne M, Urban G, Frankenberg D, Löbrich M. DNA double-strand break misrejoining after exposure of primary human fibroblasts to CK characteristic x rays, 29 kvp x rays and 60Co γ rays. Radiat Res 2005; 164:669–76.

20. Depuydt J, Baert A, Vandersickel V, Thierens H, Vral A. Relative biological effectiveness of mammography x-rays at the level of DNA and chromosomes in lymphocytes. Int J Radiat Biol 2013; 89:532–8.

21. Heyes G, Mill A. The neoplastic transformation potential of mammography x rays and atomic bomb spectrum radiation. Radiat Res 2004; 162:120–7.

22. Frankenberg D, Kelnhofer K, Bar K, Frankenberg-Schwager M. Enhanced neoplastic transformation by mammography x rays relative to 200 kvp x rays: Indication for a strong dependence on photon energy of the RBE(m) for various end points. Radiat Res 2002; 157:99–105.

23. Göggelmann W, Jacobsen C, Panzer W, Walsh L, Roos H, Schmid E. Re-evaluation of the RBE of 29 kv x-rays (mammography x-rays) relative to 220 kv x-rays using neoplastic transformation of human cgl1-hybrid cells. Radiat Environ Biophys 2003; 42:175–82.

24. Schmid E. Is there reliable experimental evidence for a low-dose RBE of about 4 for mammography x rays relative to 200 kv x rays? Radiat Res 2002; 158:778–81.

25. Gomolka M, Rössler U, Hornhardt S, Walsh L, Panzer W, Schmid E. Measurement of the initial levels of DNA damage in human lymphocytes induced by 29 kv x rays (mammography x rays) relative to 220 kv x rays and γ rays. Radiat Res 2005; 163:510–9.

26. Brenner DJ, Sawant SG, Hande MP, Miller RC, Elliston CD, Fu Z, et al. Routine screening mammography: How important is the radiation-risk side of the benefit-risk equation? Int J Radiat Biol 2002; 78:1065–7.

27. Mestres M, Caballín M, Barrios L, Ribas M, Barquinero J. RBE of x rays of different energies: A cytogenetic evaluation by fish. Radiat Res 2008; 170:93–100.

28. Lehnert A, Lessmann E, Pawelke J, Dörr W. RBE of 25 kv x-rays for the survival and induction of micronuclei in the human mammary epithelial cell line MCF-12A. Radiat Environ Biophys 2006; 45:253–60.

29. Beyreuther E, Dörr W, Lehnert A, Lessmann E, Pawelke J. Relative biological effectiveness of 25 and 10 kv x-rays for the induction of chromosomal aberrations in two human mammary epithelial cell lines. Radiat Environ Biophys 2009; 48:333–40.

30. Panteleeva A, Slonina D, Brankovic K, Spekl K, Pawelke J, Hoinkis C, et al. Clonogenic survival of human keratinocytes and rodent fibroblasts after irradiation with 25 kv x-rays. Radiat Environ Biophys 2003; 42:95–100.

31. Frankenberg-Schwager M, Garg I, Frankenberg D, Greve B, Severin E, Uthe D, et al. Mutagenicity of low-filtered 30 kvp x-rays, mammography x-rays and conventional x-rays in cultured mammalian cells. Int J Radiat Biol 2002; 78:781–9.

32. Virsik RP, Harder D, Hansmann I. The RBE of 30 kv x-rays for the induction of dicentric chromosomes in human lymphocytes. Radiat Environ Biophys 1977; 14:109–21.

33. Slonina D, Spekl K, Panteleeva A, Brankovic K, Hoinkis C, Dörr W. Induction of micronuclei in human fibroblasts and keratinocytes by 25 kv x-rays. Radiat Environ Biophys 2003; 42:55–61.

34. Redpath JL, Mitchel RE. Enhanced biological effectiveness of low energy x-rays and implications for the uk breast screening programme. Br J Radiol 2006; 79:854–5; Author reply 855–7.

35. Ko S, Liao X, Molloi S, Elmore E, Redpath J. Neoplastic transformation in vitro after exposure to low doses of mammographic-energy x rays: Quantitative and mechanistic aspects. Radiat Res 2004; 162:646–54.

36. Portess DI, Bauer G, Hill MA, O'Neill P. Low-dose irradiation of nontransformed cells stimulates the selective removal of precancerous cells via intercellular induction of apoptosis. Cancer Res 2007; 67:1246–53.

37. Beels L, Werbrouck J, Thierens H. Dose response and repair kinetics of γ-H2AX foci induced by in vitro irradiation of whole blood and T-lymphocytes with x- and γ-radiation. Int J Radiat Biol 2010; 86:760–8.

38. Colin C, Devic C, Noel A, Rabilloud M, Zabot MT, Pinet-Isaac S, et al. DNA double-strand breaks induced by mammographic screening procedures in human mammary epithelial cells. Int J Radiat Biol 2011; 87: 1103–12.

39. Grudzenski S, Raths A, Conrad S, Rube CE, Lobrich M. Inducible response required for repair of low-dose radiation damage in human fibroblasts. Proc Natl Acad Sci U S A 2010; 107:14205–10.

40. Rothkamm K, Krüger I, Thompson LH, Löbrich M. Pathways of DNA double-strand break repair during the mammalian cell cycle. Mol Cell Biol 2003; 23:5706–15.

41. Asaithamby A, Chen DJ. Cellular responses to DNA double-strand breaks after low-dose gamma-irradiation. Nucleic Acids Res 2009; 37:3912–23.